

A Study of Parton Energy Loss in Au+Au Collisions at RHIC using Transport Theory

Y. Nara

RIKEN-BNL Research Center, Brookhaven National Laboratory, Upton, NY

S.E. Vance

Physics Department, Brookhaven National Laboratory, Upton, NY

P. Csizmadia

RMKI Research Institute for Particle and Nuclear Physics, Budapest, Hungary

Parton energy loss in Au+Au collisions at RHIC energies is studied by numerically solving the relativistic Boltzmann equation for the partons including $2 \leftrightarrow 2$ and $2 \rightarrow 2 +$ final state radiation collision processes. Final particle spectra are obtained using two hadronization models; the Lund string fragmentation and independent fragmentation models. Recent, preliminary π^0 transverse momentum distributions from central Au+Au collisions at RHIC are reproduced using gluon-gluon scattering cross sections of 5 – 12 mb, depending upon the hadronization model. Comparisons with the HIJING jet quenching algorithm are made.

25.75.-q, 12.38.Mh, 24.85.+p, 13.87.-a

Exciting, preliminary π^0 transverse momentum distributions from Au+Au collisions at $\sqrt{s_{NN}} = 130$ GeV at RHIC have been recently reported [1,2]. When normalized to the mean number of binary collisions, the ratio of the central to the peripheral distributions increases up to $p_T \sim 2$ GeV/c, reaches a maximum value that is less than 1 and then decreases for $p_T > 2$ GeV. This preliminary data reveals a suppression of the production of π^0 s in central Au+Au collisions for $p_T > 2$ GeV/c.

The preliminary π^0 transverse momentum distribution has been reproduced by several calculations that included jet quenching [3,4]. Jet quenching occurs when a high energy jet passes through a medium and loses energy from the induced non-abelian radiation. Recently, intense theoretical activity has been devoted to calculating the energy loss of a fast parton traveling through QCD media [5–8]. It has been shown that transverse momentum distributions of hadrons at large p_T are sensitive to the total energy loss of the fast partons [9]. Jet quenching has been proposed as one of the signals of the formation of a quark-gluon plasma (QGP) [9–11]. Recent pQCD motivated calculations that include the nuclear effects of shadowing and energy loss via a modified fragmentation function have shown that the π^0 data can be reproduced with a constant energy loss of $dE/dz = 0.25$ GeV/fm [3]. Using a similar approach, but with a dE/dz that depends upon the number of collisions, it was shown that the data can also be reproduced with $\bar{n} = 3 - 4$ average number of scatterings [4].

While there have been many theoretical studies of jet quenching, few simulation models have incorporated this physics. The HIJING simulation model [12] and the two other models which use the HIJING algorithms, such as HIJING/B \bar{B} [13] and AMPT [14] incorporate a simple jet quenching mechanism. The HIJING jet quenching algorithm [12] assumes a simple gluon splitting scheme with a

fixed energy loss dE/dz . The energy loss for gluon jets is twice that of the quark jets. A jet can only interact with locally comoving matter (strings) in the transverse direction and the points of the interactions are determined by the probability $dP(l) = dl/\lambda e^{-l/\lambda}$, where λ is the mean free path and l is the distance the jet has traveled between collisions. When an interaction occurs (with a string), the medium induced radiation is simulated by forming a gluon kink in the string with $\Delta E = ldE/dz$ of the jets energy. A jet can interact with the surrounding medium until it exits the system or its p_T fall below a certain p_0 cut-off. As the energy of a nuclear collision increases, more partons are produced, and this jet quenching algorithm leads to the production of many additional low energy gluons (gluon kinks). In a default HIJING jet quenching calculation with $dE/dz = 2$ GeV/fm, the charged hadron multiplicity per participant was shown to increase with the colliding energy much faster than the data [15–17].

The effects of the parton scattering phase where only elastic parton interactions are included have been studied with several models; ZPC [18], AMPT [14,19], MPC [20] and GROMIT [21]. Calculations revealed [19] that elastic parton interactions only slightly decrease the E_T and multiplicity and produce very little elliptic flow when typical gluon-gluon pQCD cross section of $\sigma_{gg} \sim 3$ mb and $dN_g/dy|_{y=0} \sim 200$ are used. A large elliptic flow is only obtained when gross cross sections or large gluon densities are used [20]. Inelastic processes, like $gg \leftrightarrow ggg$, have been shown to be important [22–24] for thermalizing the partons and in the radiative energy loss of the high energy jets.

In this work, a model is introduced that describes the parton scattering phase for high energy heavy ion collisions by numerically solving the Boltzmann equation for a distribution of partons with $2 \leftrightarrow 2$ and

$2 \rightarrow 2$ + final state radiation interactions. The $2 \rightarrow 2$ + final state radiation processes are needed to effectively simulate jet quenching and the dynamical scatterings of the partons lead to a reduction of the E_T at mid-rapidity. As a result, the incident energy dependence of the multiplicity per participant in this approach is similar to HIJING without jet quenching and is consistent with data [16,17].

The initial parton distributions in our model are obtained from the HIJING event generator which produces around 190 gluons at mid-rapidity for a typical Au+Au collision at $\sqrt{s_{NN}} = 130$ GeV. The nuclear shadowing effects in HIJING are included in all calculations in this paper. The system of partons is then evolved in time using the relativistic Boltzmann equation,

$$p^\mu \partial_\mu f(x, p) = C, \quad (1)$$

where $f(x, p)$ is the distribution function of the partons and C is the collision integral. For the collision integral, $2 \leftrightarrow 2$ and $2 \rightarrow 2$ + final state radiation processes are included. The distribution function, $f(x, p)$ is assumed to be the sum of the particles,

$$f(x, p) = \frac{1}{N_{test}} \sum_{i=1}^{AN_{test}} \delta(x_i - x) \delta(p_i - p), \quad (2)$$

where N_{test} is the number of “test particles” and A is the actual number of partons produced in a collision. The momentum of the partons is determined by HIJING and the space-time coordinates are calculated using simple uncertainty relations. The formation time for partons is taken to be a Lorentzian distribution with a half width $t = E/m_T^2$, where E and m_T are the parton energy and transverse mass, respectively [19].

Monte-Carlo simulation is used to solve the Boltzmann equation. In this simulation, the on-shell partons are evolved in time along straight lines between collisions, where all of the collisions are time-ordered in a global frame. After each collision, the flavor, position and momentum of the outgoing partons are determined and the list of possible collisions is updated. The space-time evolution of the system continues until there are no possible collisions between the partons.

The “parallel-ensemble” method has been widely used to simulate the low energy nucleus-nucleus collisions [25]. In this method, collisions are determined using the “closest distance approach”, where a collision occurs if the minimum relative distance b_{rel} for any pair of particles in their center of mass frame becomes less than interaction range as given by $\sqrt{\sigma/\pi}$. Here, σ is the total parton-parton cross section. However, this method violates Lorentz invariance due to the nature of action at a distance; a problem that has been studied by several authors [18,20,21,26]. Two solutions to this problem have been proposed. The “full-ensemble” method replaces each particle by N_{test} particles that interact with a reduced cross section σ/N_{test} [20,27,28]. In the

limit of $N_{test} \rightarrow \infty$, one obtains the locality in configuration space. Another solution is the “local-ensemble” method [29,30] where the probability for one pair of the test particles to collide during the time interval of Δt in the small volume element ΔV is given by

$$W = \sigma v \Delta t / (N_{test} \Delta V). \quad (3)$$

Here v is the relative velocity of the scattering particles. In the limit of $\Delta V \rightarrow 0$, $\Delta t \rightarrow 0$, $N_{test} \rightarrow \infty$, the solutions will converge to the exact solutions of the Boltzmann equation. In this study, the full-ensemble method is used with $N_{test} = 6$.

The parton-parton interactions included in this simulation are

$$\begin{aligned} q + q' &\leftrightarrow q + q', & g + g &\leftrightarrow g + g, \\ g + g &\leftrightarrow q + \bar{q}, & g + q &\leftrightarrow g + q. \end{aligned} \quad (4)$$

The cross sections for these processes are given by leading order (LO) perturbative QCD (LOpQCD) [31] and explicitly take into account the running coupling constant $\alpha_s(Q^2)$. Here, the Q^2 scale is chosen to be the squared transverse momentum transfer of the scattering process $Q^2 = p_T^2$ and $\alpha_s(Q^2)$ is evaluated at the scale of 1 GeV², when $p_T < 1$ GeV. Since these cross sections diverge when $p_T \rightarrow 0$, a Debye screening mass $m_D = 0.6$ GeV [18] and quark thermal mass $m_q = 0.2$ GeV are introduced to regulate the propagators [26,24]. While these values should change with time, they are taken to be constant for simplicity. In this paper, two sets of results are obtained by multiplying these cross sections with two different factors (K -factors); $K = 1.0$ and $K = 2.5$. For example, a K -factor of 1.0 yields $\sigma_{gg} \sim 5.3$ mb for the gluon-gluon cross section, $\sigma_{gq} \sim 2.0$ mb for the quark-gluon, and $\sigma_{qq} \sim 0.5$ mb for the quark-quark, and a K -factor of 2.5 yields 2.5 times the values for $K = 1$.

The $2 \rightarrow 2$ + final state radiation processes are modeled using PYTHIA algorithms [32], where the two outgoing partons are evolved with time-like branching taking into account angular ordering. This approach has been used to study the gluon jet production in e^+e^- interactions. During the branching, the life times of newly branched partons are obtained using the uncertainty principle, $t_{form} \sim 1/Q$, where Q represents the off-shellness of the parton in its rest frame [33]. The minimum virtuality for the final state radiation is chosen to be 0.5 GeV [33]. The number of emitted gluons (amount of final state radiation) is sensitive to this cutoff parameter. Using a $Q^2 = 1$ GeV² with $K = 2.5$ yielded less final state radiation and hence less energy loss. A systematic study will be given later. The maximum virtuality in parton-parton scattering is assumed to be $Q_{max}^2 = 4p_T^2$, where p_T is the transverse momentum transfer of the scattering process. Off-shell partons are not allowed to interact with other partons in the system. While the final state (time-like) radiation is occurring, possible interactions with other partons are ignored, in contrast to the parton cascade model VNI [22].

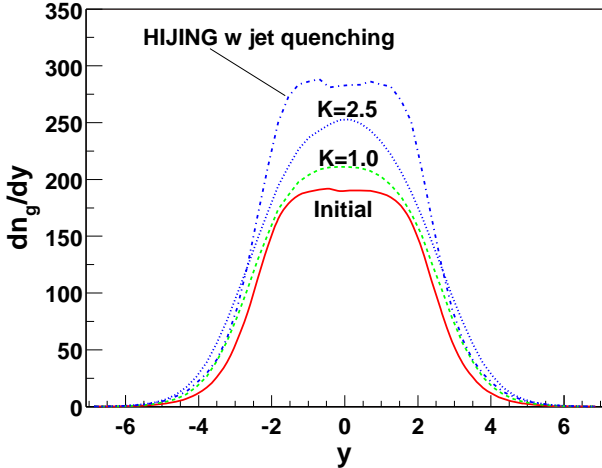


FIG. 1. Rapidity distributions of mini-jet gluons for $Au + Au$ collisions ($b < 4.48$ fm) at $\sqrt{s_{NN}} = 130$ GeV. The solid line denotes the distribution from the initial condition (HIJING no jet quenching), and the dashed and dotted line represent the distributions after rescattering with a K factor of 1.0 and 2.5 respectively. The dotted-dashed line is the result from HIJING default calculation ($dE/dz = 2.0$ GeV/fm).

In Fig. 1, the rapidity distributions of the mini-jet gluons for central $Au+Au$ collisions at $\sqrt{s_{NN}} = 130$ GeV are shown. The solid curve represents the initial rapidity distribution of gluons obtained from the HIJING model without jet quenching; $dN/dy_{g,y=0} = 190$. With this initial distribution, the dynamical evolution of the partons with $2 \rightarrow n$ interactions enhances the gluon multiplicity, where $dN/dy_{g,y=0} = 210$ for $K = 1.0$, and $dN/dy_{g,y=0} = 250$ for $K = 2.5$. In comparison, HIJING with jet quenching with $dE/dz = 2.0$ GeV/fm yields 280 gluons near mid-rapidity. As observed, these values are sensitive to the magnitude of the parton-parton cross sections.

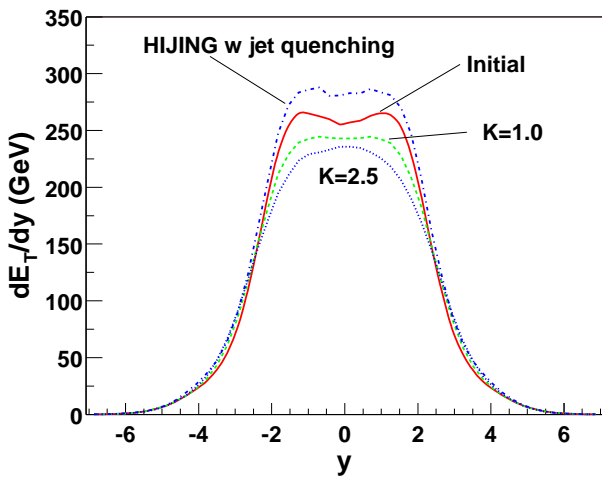


FIG. 2. Transverse energy rapidity distributions of partons for $Au+Au$ collisions ($b < 4.48$ fm) at $\sqrt{s_{NN}} = 130$ GeV. The solid line denotes the distribution from the initial condition and the dashed ($K = 1.0$) and dotted ($K = 2.5$) line represents the distributions after rescattering. HIJING with default jet quenching result is shown by the dotted-dashed line.

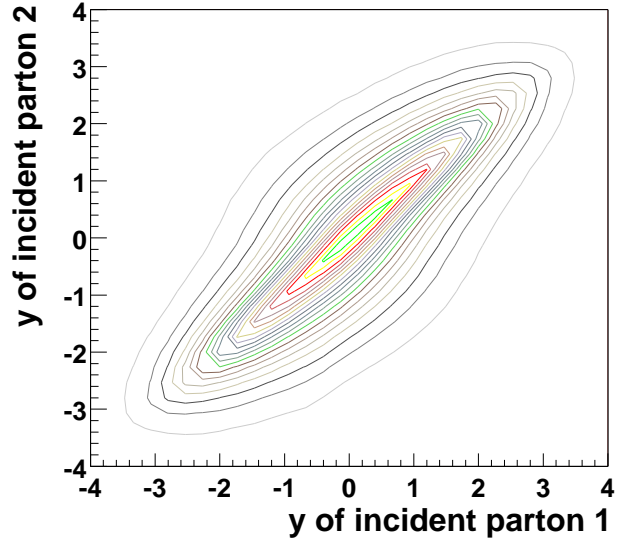


FIG. 3. Rapidity correlation for parton-parton scattering for $Au+Au$ collisions ($b < 4.48$ fm) at $\sqrt{s_{NN}} = 130$ GeV. $K = 2.5$ is used.

In Fig. 2, the rapidity distributions of mini-jet transverse energy dE_T/dy in central $Au+Au$ collisions at $\sqrt{s_{NN}} = 130$ GeV is shown. After the partons are dynamically evolved, the dE_T/dy of the partons is reduced by approximately 13 GeV for $K = 1.0$ and 27 GeV for $K = 2.5$. The loss in E_T results from the strong rapidity correlation in the parton-parton collisions. The rapidity correlation for the case of $K = 2.5$ is plotted in Fig. 3. As the partons with similar rapidities collide, the momentum is redistributed from transverse to longitudinal and the E_T decreases. The degree of the correlation depends on the parton-parton cross sections, where the correlation becomes stronger as the cross sections decrease. Most collisions in the simulation occur around the $p_T \sim 1.0$ GeV/c. In comparison, in Fig. 2, the HIJING jet quenching scheme increases the dE_T/dy . In the HIJING jet quenching scheme, the medium induced radiation is simulated by forming a *collinear* gluon (kink in the string). In this approach, little of the transverse momenta is redistributed.

Fig. 4 shows the gluon transverse momentum distributions from our calculations at the $\sqrt{s_{NN}} = 130$ GeV for central $Au+Au$ collisions together with HIJING jet quenching calculations. The inclusion of $2 \rightarrow 2 +$ final state radiation processes results in the reduction of high p_T partons and a slight increase in the low $p_T < 1$ GeV region. This effect is sensitive to the size of

the parton-parton cross sections and the assumed energy loss dE/dz .

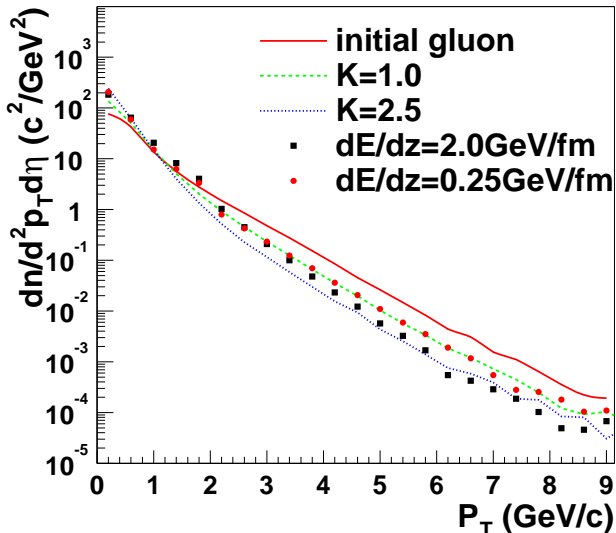


FIG. 4. Transverse momentum distributions of gluons for $Au + Au$ collisions ($b < 4.48$ fm) at $\sqrt{s_{NN}} = 130$ GeV. The solid line denotes the distribution from the initial condition and the dashed and dotted lines represent the distributions after rescattering with $K = 1.0$ and $K = 2.5$, respectively. HIJING results are also shown in squares ($dE/dz = 2.0$ GeV/fm) and circles ($dE/dz = 0.25$ GeV/fm).

Once the partons have finished interacting, two different hadronization models are used to obtain the hadron spectra; the Lund string fragmentation and independent fragmentation models. The results of these two models are compared with one another and with the π^0 data.

When using the Lund string fragmentation model [32], the string configurations are maintained throughout the evolution of the partonic system by determining the string configuration from the color amplitude of each parton-parton collision. In the PYTHIA manual [31], detailed explanations of the possible string configurations for the relevant parton-parton scattering processes are provided.

As shown in Fig. 5, the HIJING without jet quenching calculation (solid line) overestimates the data at $p_T > 2$ GeV/c as consistent with other pQCD motivated parton model calculations [2,3]. Jet quenching is not seen in the low p_T region, $1 < p_T < 2$ GeV/c, as expected. As a result of the dynamical evolution of the partons, the data can be reproduced with the $K = 2.5$ cross section set. In addition, HIJING with jet quenching $dE/dz = 0.25 - 2.0$ GeV/fm is able to reproduce the data. The dominant contribution of the π^0 with $p_T \approx 2-4$ GeV/c comes from the hadronization of quarks with $p_T > 4$ GeV/c. Thus, the π^0 distribution is sensitive to the energy loss of the quarks and it is very important to include the appropriate qq and qg interactions.

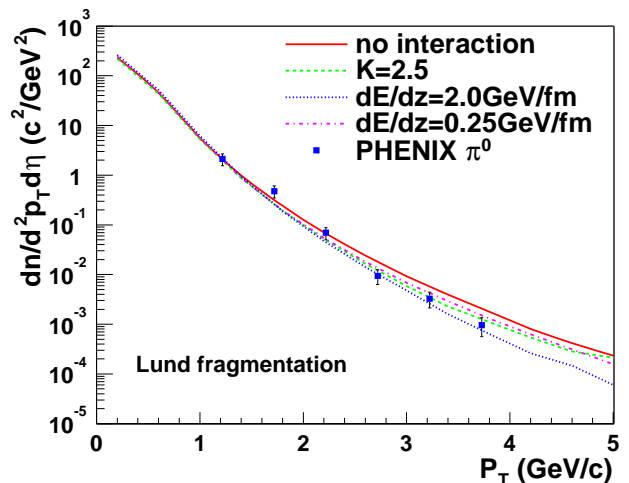


FIG. 5. A comparison of neutral pion transverse momentum distributions for central $Au + Au$ collisions ($b < 4.48$ fm) at $\sqrt{s_{NN}} = 130$ GeV with the PHENIX data [2] is presented. The solid line denotes the distribution from the initial condition and the dashed line represents the gluon distribution after rescattering with the K factor of 2.5. The HIJING results for $dE/dz = 2.0$ GeV/fm (dotted line) and $dE/dz = 0.25$ GeV/fm (dotted-dashed line) are also shown.

Since explicit local color connections are not believed to be maintained in a high density partonic system, the independent fragmentation model is also used to compute the final hadron spectra. The independent fragmentation model fragments all of the partons independently. As compared to the Lund string model, this model does not incorporate long range correlations between the partons. Within this hadronization scheme, the high p_T π^0 data can be reproduced with $K = 1.0$ as shown in Fig. 6. Not shown is a calculation with $K = 2.5$ which had a larger energy loss, underestimating the data. Since the long-range correlations between partons are absent, the final hadron distribution strongly reflects the parton distribution. Changing the fragmentation model in HIJING from the default Lund string model to the independent fragmentation model, the HIJING calculations with jet quenching show similar behavior. Above $p_T > 2.0$ GeV/c, calculations assuming $dE/dz = 0.25$ GeV/fm are able to reproduce the data. This value is the same as that obtained from the pQCD motivated parton model calculations [3].

The total hadron yields from our model near mid-rapidity are smaller than the HIJING *without* jet quenching values by approximately 4% when using Lund string fragmentation model and are larger by approximately 2% when using the independent fragmentation model. We have checked that the model yields similar results at $\sqrt{s_{NN}} = 200$ GeV. Our calculations are therefore consistent with data [17] on the energy dependence of the hadron yield near mid-rapidity.

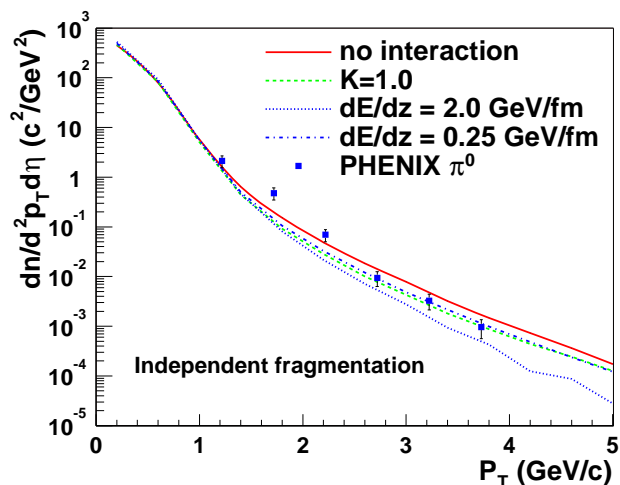


FIG. 6. A comparison of neutral pion transverse momentum distributions for central $Au + Au$ collisions ($b < 4.48$ fm) at $\sqrt{s_{NN}} = 130$ GeV with the PHENIX data [2] is presented. The solid line denotes the distribution from the initial condition and the dashed line represents the distribution after rescattering using $K = 1$. The HIJING calculations (independent fragmentation model used) with jet quenching for $dE/dz = 2.0$ GeV/fm (dotted line) and $dE/dz = 0.25$ GeV/fm (dotted-dashed line) are also shown.

In this paper, we study parton energy loss in central $Au+Au$ collisions at RHIC by numerically solving the Boltzmann equation with $2 \leftrightarrow 2$ and $2 \rightarrow 2 +$ final state radiation parton processes. Preliminary data on the π^0 p_T distributions at RHIC were fit with gluon-gluon cross sections of 5-12 mb, depending upon the hadronization model. This approach provides the maximum incoherent bound for energy loss in comparison to the LPM effect.

With the given HIJING initial condition, the parton scatterings reduce the parton $dE_T/dy|_{y=0}$ by 5-10%. The magnitude of the change in the E_T is sensitive to the scattering cross section. Interactions between particles that are strongly correlated in rapidity lead to a redistribution of the momenta from the transverse to the longitudinal direction and are important in lowering the E_T and the final hadron multiplicity. Similar effects have been pointed out in regard to the suppressed production of open charm in the pre-equilibrium stage [34].

To test the sensitivity of the π^0 spectra to the non-perturbative hadronization process, two different hadronization schemes were used. Larger parton-parton scattering cross sections were needed to reproduce the π^0 distributions when using Lund string fragmentation than when using independent fragmentation. The spectra produced by independent fragmentation are more sensitive to changes in the parton distributions, due to the lack of the long-range correlations introduced by the strings. These two different hadronization schemes therefore require different amounts of parton energy loss in order to reproduce the data.

While we have investigated the energy loss in the par-

ton scattering phase, future calculations should also address the change in the p_T distributions of the particles from the late hadron gas stage. The effect of the parton scattering phase using other initial conditions [35–39] should also be explored.

We would like to thank S. Cheng, M. Gyulassy, P. Levai and I. Vitev for their helpful comments. This manuscript was authored under Contract No. DE-AC02-98CH10886 with the U. S. Department of Energy and by Hungarian OTKA Grant T025579.

-
- [1] K. Adcox, PHENIX Collaboration, nucl-ex/0109003.
 - [2] G. David, PHENIX Collaboration, nucl-ex/0105014. Talk given at 15th International Conference on Ultrarelativistic Nucleus-Nucleus Collisions (QM2001), Stony Brook, New York, 15-20 Jan 2001. Submitted to Nucl. Phys. A.
 - [3] X.-N. Wang, nucl-th/0105053. Talk given at 15th International Conference on Ultrarelativistic Nucleus-Nucleus Collisions (QM2001), Stony Brook, New York, 15-20 Jan 2001. Submitted to Nucl. Phys. A.
 - [4] P. Levai, et al., nucl-th/0104035. Talk given at 15th International Conference on Ultrarelativistic Nucleus-Nucleus Collisions (QM2001), Stony Brook, New York, 15-20 Jan 2001. Submitted to Nucl. Phys. A.
 - [5] R. Baier, Yu.L. Dokshitzer, A.H.Mueller, S. Peigne and D. Schiff, *Nucl. Phys. B* **483**, 291 (1997); *Nucl. Phys. B* **484**, 265 (1997); *Nucl. Phys. B* **531**, 403 (1998).
 - [6] B.G. Zakharov, *JEPT* **63**, 952 (1996); *JEPT* **63**, 615 (1997).
 - [7] U.A. Wiedemann, *Nucl. Phys. A* **690**, 731 (2001); *Nucl. Phys. B* **588**, 393 (2000); U.A. Wiedemann and M. Gyulassy, *Nucl. Phys. B* **560**, 345 (1999).
 - [8] M.Gyulassy, P. Levai and I. Vitev, *Nucl. Phys. B* **594**, 371 (2001) *Phys. Rev. Lett.* **85**, 5535 (2000) *Nucl. Phys. B* **571**, 197 (2000)
 - [9] X.-N Wang and M. Gyulassy, *Phys. Rev. Lett.* **68**, 1480 (1992).
 - [10] M. Gyulassy and X.-N Wang, *Nucl. Phys. B* **420**, 583 (1994); X.-N. Wang, M. Gyulassy and M. Plumer, *Phys. Rev. D* **51**, 3436 (1995).
 - [11] M. Gyulassy and M. Plumer, *Phys. Lett. B* **243**, 432 (1990).
 - [12] X.-N. Wang and M. Gyulassy, *Phys. Rev. D* **44**, 3501 (1991); X.-N. Wang, *Phys. Rep.* **280**, 287 (1997); X.-N. Wang and M. Gyulassy, *Comp. Phys. Comm.* **83**, 307 (1994).
 - [13] S. E. Vance, M. Gyulassy and X.-N. Wang, *Phys. Lett. B* **443**, 45 (1998); S. E. Vance and M. Gyulassy, *Phys. Rev. Lett.* **83**, 1735 (1999).
 - [14] Z. Lin, S. Pal, C. M. Ko, B. Li and B. Zhang, *Phys. Rev. C* **64**, 011902 (2001).
 - [15] X.-N. Wang and M. Gyulassy, *Phys. Rev. Lett.* **86**, 3496 (2001).

- [16] B. B. Back, *et al.*, PHOBOS Collaboration, *Phys. Rev. Lett.* **85**, 3100 (2000).
- [17] B. B. Back, *et al.*, PHOBOS Collaboration, nucl-th/0108009.
- [18] B. Zhang, *Comp. Phys. Comm.* **109**, 70 (1997); <http://nt1.phys.columbia.edu/people/bzhang/ZPC/zpc.html>; B. Zhang and Y. Pang, *Phys. Rev. C* **56**, 2185 (1997); B. Zhang, M. Gyulassy and Y. Pang, *Phys. Rev. C* **58**, 1175 (1998).
- [19] B. Zhang, C. M. Ko, Bao-AN Li, and Z. Lin, *Phys. Rev. C* **61**, 067901 (2000).
- [20] D. Molnar and M. Gyulassy, *Phys. Rev. C* **62**, 054907 (2000); nucl-th/0104073.
- [21] S. Cheng *et al.*, nucl-th/0107001.
- [22] K. Geiger, *Phys. Rep.* **258**, 238 (1995); *Comp. Phys. Comm.* **104**, 70 (1997).
- [23] E. Shuryak and L. Xiong, *Phys. Rev.* **C49**, 2241 (1994); T. S. Biro, E. van Doorn, B. Müller, M. H. Thoma and X.-N. Wang, *Phys. Rev. C* **48**, 1275 (1993); S. M. Wong, *Nucl. Phys. A* **607**, 442 (1996); R. Baier, A. H. Mueller, D. Schiff and D. T. Son, *Phys. Lett. B* **502**, 51 (2001).
- [24] S. M. Wong, *Phys. Rev. C* **54**, 2588 (1996).
- [25] G. F. Bertsch and S. Das Gupta, *Phys. Rep.* **150**, 189 (1988).
- [26] G. Kortemeyer, W. Bauer, K. Haglin, J. Murray and S. Pratt, *Phys. Rev. C* **52**, 2714 (1995).
- [27] G. Welke, R. Malfliet, C. Grégoire, M. Prakash, and E. Suraud, *Phys. Rev. C* **40**, 2611 (1989).
- [28] A. Lang, W. Cassing, U. Mosel, and K. Weber, *Nucl. Phys. A* **541**, 507 (1992).
- [29] A. Lang, H. Babovsky, W. Cassing, U. Mosel, H.G. Reusch and K. Weber, *J. Comp. Phys.* **106**, 391 (1993).
- [30] P. Danielewicz and G. F. Bertch, *Nucl. Phys.* **A533**, 712 (1991).
- [31] H.-U Bengtsson, *Comp. Phys. Comm.* **31**, 323 (1984).
- [32] T. Sjöstrand, *Comp. Phys. Comm.* **82**, 74 (1994); PYTHIA 5.7 and JETSET 7.4 Physics and Manual. <http://thep.lu.se/tf2/staff/torbjorn/Welcome.html>.
- [33] K. J. Eskola, X.-N. Wang, *Phys. Rev. D* **49**, 1284 (1994).
- [34] Z. Lin and M. Gyulassy, *Phys. Rev. C* **51**, 2177 (1995); P. Lévai, B. Müller and X.-N Wang, X.-N. Wang, *Phys. Rev. C* **51**, 3326 (1995).
- [35] K. J. Eskola, K. Kajantie, P. V. Ruuskanen and K. Tuominen, *Nucl. Phys. B* **570**, 379 (2000); K. J. Eskola, K. Kajantie and K. Tuominen, *Phys. Lett. B* **497**, 39 (2001).
- [36] A. H. Mueller, *Nucl. Phys. B* **558**, 285 (1999); A. H. Mueller, *Nucl. Phys. B* **572**, 227 (2000); D. Kharzeev and M. Nardi, *Phys. Lett.* **B507** (2001), 121; D. Kharzeev and E. Levin, nucl-th/0108006.
- [37] L. McLerran and R. Venugopalan, *Phys. Rev.* **D49** 2233 (1994); **D49** 3352 (1994); **D50** 2225 (1994).
- [38] A. Krasnitz, and R. Venugopalan, *Nucl. Phys. B* **557**, 237 (1999); *Phys. Rev. Lett.* **84** (2000) 4309; *Phys. Rev. Lett.* **86** (2001) 1717; A. Krasnitz, Y. Nara and R. Venugopalan, hep-ph/0108092.
- [39] Z. Lin and C. M. Ko, nucl-th/0108039.